THE AMERICAN SOCIETY OF MECHANICAL ENGINEERS
345 E. 47th St., New York, N.Y. 10017

98-GT-572

The Society shall not be responsible for statements or opinions advanced in papers or discussion at meetings of the Society or of its Divisions or Sections, or printed in its publications. Discussion is printed only if the paper is published in an ASME Journal. Authorization to photocopy for internal or personal use is granted to libraries and other users registered with the Copyright Clearance Center (CCC) provided $3/article or $4/page is paid to CCC, 222 Rosewood Dr., Danvers, MA 01923. Requests for special permission or bulk reproduction should be addressed to the ASME Technical Publishing Department.

Copyright © 1998 by ASME All Rights Reserved Printed in U.S.A.

THE INFLUENCE OF TAILBOARDS ON UNSTEADY MEASUREMENTS IN A LINEAR CASCADE

P. Ott, M. Norryd, A. Bölcs

Laboratoire de Thermique Appliquée et de Turbomachines (LTT)
Swiss Federal Institute of Technology
1015 Lausanne, Switzerland

ABSTRACT

The present paper shows the comparison between steady-state and unsteady results from two versions of a flow solver and measurements in a linear cascade at transonic flow conditions for forced vibration of a single blade.

Experiments have been conducted in a linear test facility with a cascade composed of five turbine blades. The center blade was forced to oscillate in a pure bending mode with a frequency of 160 Hz. Tailboards are fixed in this test facility at the trailing edges of the border blades to create a periodic flow at the outlet of the cascade.

A 2D inviscid flow solver for unsteady flows through vibrating blade rows was adapted to simulate the flow conditions in the linear cascade.

The initial adaptation of the flow solver was the limitation to only one vibrating blade. Comparisons with measurements showed discrepancies which were hypothesized to be due to the presence of the tailboards which can create reflections of pressure waves and shocks.

Therefore, as a second modification of the program, the periodic boundaries downstream of the blades were replaced by solid walls.

Based on these computations it can be concluded that for transonic flows the tailboards have a significant influence on both the steady-state and unsteady flow in the outlet region as well as on the blade in the shock region. In particular, the unsteady data measured in a linear cascade has to be analyzed very carefully to estimate the influence of the tailboards.

NOMENCLATURE

c	chord length
$\tilde{c}_p$	unsteady pressure coefficient
	$\tilde{c}_p(x,t) = \frac{1}{h} \cdot \frac{\tilde{p}(x,t)}{\bar{p}_{w1} - \bar{p}_1}$
f	frequency
h	dimensionless (with chord) bending vibration amplitude
M	Mach number
p	pressure
t	time
x	coordinate
β	flow angle
δ	bending direction
φ_p	phase angle between blade movement and pressure signal

Subscripts

1	inlet values at upstream infinity
2	downstream values
s	isentropic condition
w	stagnation value

Presented at the International Gas Turbine & Aeroengine Congress & Exhibition
Stockholm, Sweden — June 2– June 5, 1998

Downloaded From: http://proceedings.asmedigitalcollection.asme.org/ on 06/19/2018 Terms of Use: http://www.asme.org/about-asme/terms-of-use

INTRODUCTION

Linear test facilities are widely used for the investigation of steady-state flow in turbine or compressor cascades. Over the years, unsteady testing has been performed in such facilities as well. Results of flutter investigations have been presented by Loiseau and Széchényi (1981), Széchényi and Girault (1981), Girault (1984), Széchényi and Cafarelli (1989).

In the present work, investigations in a linear turbine cascade with single-blade excitation were undertaken. Unsteady pressures on the surface of the vibrating blade and at the side wall of the test facility were measured.

In parallel to these investigations, blades of the same geometry were tested in an annular cascade for forced vibration in the traveling wave mode.

When comparing the behavior of both cascades some unexplained discrepancies were observed on the suction side of the blade in the linear cascade.

The analysis of the results indicated that these discrepancies could be due to reflections of pressure waves and shocks on the tailboards (see Fig. 1). Buffum and Fleeter (1993) had found similar effects and supposed the reason to be most likely reflections of acoustic waves at the solid boundaries of the test facility.

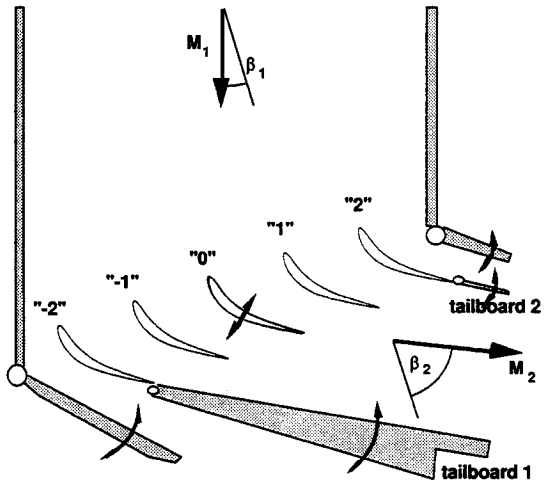

Fig. 1: Schematic view of the linear test facility

To conduct this analysis, an existing numerical code was modified to simulate the cascade flow with and without the tailboards. The differences between the results were intended to provide insight into the influence of the tailboards on the unsteady pressure field.

MEASURING EQUIPMENT

Test Facility

The linear test facility (see Fig. 1) is supplied continuously with air by a centrifugal compressor at a maximum mass flow rate of 10 kg/s and a maximum stagnation pressure of 350 kPa.

For the present work, the facility was equipped with a cascade composed of five turbine blades which have the same geometry as the new eleventh standard configuration [Bölcs and Fransson, 1986, Fransson and Verdon, 1992, Fransson et al., 1998].

The test section measures 360 mm between the leading edges of blade "-2" and blade "+2" and has a channel width of 100 mm.

The cascade is mounted on a disk which allows an easy adjustment of the inlet flow angle. At the trailing edges of blade "-2" and blade "+2" tailboards are fixed. These tailboards can be positioned to achieve flow periodicity.

For steady-state measurements, slotted tailboards are typically used in order to diminish or eliminate reflections of shocks. Behind the slotted surface, a closed box maintains a constant pressure. With this slotted tailboard construction, however, additional harmonic signals were measured by the unsteady pressure transducers. The slotted tailboards seem to create acoustic waves and thus should not be used when doing unsteady measurements. By replacing the slotted tailboards with solid ones, these unsteady disturbances were eliminated. All here presented steady-state and unsteady measurements were conducted with solid tailboards.

For unsteady measurements, the center blade "0" can be forced into controlled vibrations. An electromagnetic system fixed at the outer wall of the cascade provides controlled blade vibrations in the bending mode up to 200 Hz. The blade entry passage in the side wall of the tunnel is equipped with a specially-designed labyrinth sealing system (see Bölcs and Norryd (1994)). This system significantly reduces the effects of flow leakage through the side wall on the steady and unsteady measurements, while still ensuring an unrestricted plunging motion of the blade.

Instrumentation

Two lines of static pressure taps on the side wall in front and behind the cascade are used to check the periodicity of the flow.

Pressure taps on blade "1" are used to measure the steady-state Mach number distribution.

For the unsteady pressure measurements, the center blade "0" is equipped with miniature, high-response, piezoresistive pressure transducers. A total of 12 transducers are imbedded in the blade at mid-span, with 2 installed along the pressure side and 10 installed along the suction side. The voltage signal from each transducer is passed through a DC-filter, amplifier, and low pass filter (cut-off frequency of 1000 Hz). The calibration of the transducer, including the complete measuring chain, was performed dynamically using an oscillating reference pressure for the desired range of frequencies. For the cases in which the blade was vibrating, a correction was also added to compensate for the false pressure signal produced as a result of the acceleration of the imbedded transducers. These corrections were calculated under a no-flow condition for the excitation frequency. The systematic error on the unsteady pressure amplitudes was determined to be less than 1 %, the error on the phase angle is about 0.2°.

The blade vibration is measured by an accelerometer imbedded in the blade.

For the unsteady data acquisition, the analog data signals were digitized on a PC based system which was also used for the data reduction.

Flow Conditions

The most important influence of the tailboards was observed, as expected, for transonic flow cases. To examine numerically the influence of the presence of tailboards, a case with the following flow conditions was chosen:

Inlet flow angle:	β_1	= 10.5°
Inlet Mach number	M_1	= 0.34
Isentropic downstream Mach number	M_{2s}	= 0.94
Excitation frequency	f	= 160 Hz
Vibration amplitude	h	= 0.3 mm
Bending direction	δ	= 90 °

A good repeatability for steady-state and unsteady results for these flow conditions can be stated.

Downloaded From: http://proceedings.asmedigitalcollection.asme.org/ on 06/19/2018 Terms of Use: http://www.asme.org/about-asme/terms-of-use

NUMERICAL TOOL

The computational method presented here is an explicit, inviscid two-dimensional finite-difference method of second order accuracy, based on the Euler equations in conservative form. The space integration is done by an upwinding model using the Flux-Vector-Splitting method of van Leer [Anderson et al., 1987].

The model has been extended from a previous work [Ott et al., 1995]. Only the details of the modifications made to this model for the present work are described here:

The previous model was designed to compute transonic nozzle flows. In order to compute turbomachinery blade rows, periodic boundaries at the upstream and downstream of the blades were introduced.

All blades can be vibrated either in bending or torsional motion with fixed interblade phase angles.

The integration in time can be realized by either the two-step predictor-corrector method of MacCormack or a recently included four-step Runge-Kutta method.

For boundary treatment at the inlet and outlet the so-called "capacitive boundary condition" is used. A perturbation impinging on one of these boundaries is reflected back into the flow field. The flow variables on these borders are determined by the method of characteristics. At the inlet, the stagnation pressure, the stagnation temperature and the flow angle are specified, and at the outlet boundary the static pressure is imposed.

Adaptation of the Solver

The solver was adapted to match the geometry and the blade vibration mode of the test facility.

A first adaptation was made by creating a cascade composed of 5 blades (4 blade channels). Periodic boundary conditions at the upstream and downstream lateral boundaries were used. The outlet flow direction was not prescribed. Only the middle blade (blade "0") was vibrated in a bending motion. This setup does not simulate exactly a single-blade vibration, but instead represents an infinite cascade with every fourth blade vibrating. Measurements in an annular cascade composed of blades with the same profile had previously shown that the influence of a vibrating blade which is situated at a distance of more than two blade channels from the measuring blade can be neglected [Schläfli, 1989]. This means that the vibration of the blade "+4" and "-4" can be neglected and the modeled flow corresponds closely to a single-blade vibration case.

The second adaptation was the modeling of the tailboards. The boundary conditions at the downstream lateral boundaries were switched from periodic to solid wall conditions. The angle of both side walls (tailboards) was set to the mean outlet flow angle found by the computation with the periodic boundary condition in the downstream zone.

Numerical Grid

Four blade channels were modeled with a H-mesh of 210 points in the streamwise direction and 40 mesh points in the orthogonal direction for each channel. The distribution of the mesh points is equidistant. The first and last rows of points in each channel are situated half of a mesh distance from the surface of the blades. The length of the inlet region is half of the axial chord length, the outlet region is twice the axial chord length.

Comparison with Other Flow Solvers

The presented flow case was also computed with two other methods, assuming periodic downstream lateral flow boundaries: FINSUP, a potential flow solver (Rolls Royce, 1987) and UNSFLO, a coupled Navier Stokes / Euler solver (Rolls Royce, 1991), using non-reflecting boundary conditions at the outlet boundary. The numerical mesh for the FINSUP computations contained 591 mesh points per channel, the mesh for UNSFLO was composed of 6872 mesh points. The mesh sensitivity was investigated for all solvers. The steady-state and the unsteady results are almost identical when using an even finer grid. Fig. 2 shows the steady-state results for all three numerical methods.

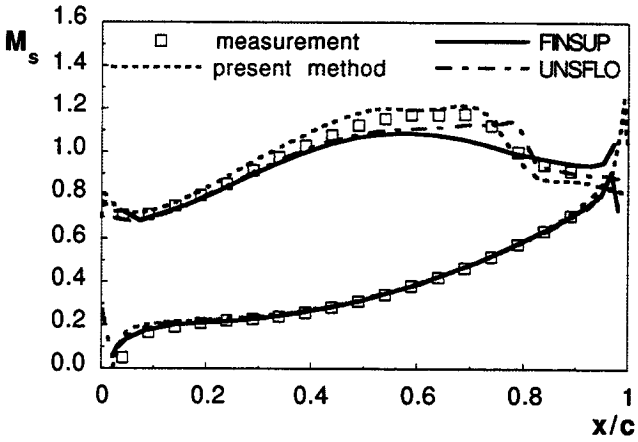

Fig. 2: Isentropic blade surface Mach number on blade "0" for measurement and all three flow solvers

All three program versions find an identical velocity distribution on the pressure side. On the suction side, however, quite important differences occur: The FINSUP flow reaches a much smaller maximum Mach number than the other solvers and seems not to calculate a shock. The two other solvers find the shock at a similar position, with UNSFLO slightly closer to the trailing edge than the here presented Euler solver. UNSFLO reaches smaller flow speeds on the suction side than the Euler solver. The comparison with the measured blade surface Mach numbers shows that the solution found with the present flow solver matches best the measured flow speed.

Figs. 3 and 4 show the comparison of the unsteady results for all three methods. All three solvers obtain very similar solutions on the pressure side.

On the suction side, some discrepancies occur: FINSUP does not show the effects of a shock in the pressure amplitude, nor the phase angle evolution. The level of pressure amplitude of FINSUP and UNSFLO are very similar, the present solver shows smaller values. UNSFLO and the present solver observe the shock similar to the steady-state solution at only slightly different positions. The phase angle shows an almost identical evolution for UNSFLO and the present solver with exception of the shock region, since UNSFLO captures the shock surprisingly sharply for a Navier-Stokes solver.

It can be concluded that the present solver shows a good agreement with other validated solvers and also the measurements, with exception of the magnitude of the unsteady pressure amplitude which is underestimated.

Downloaded From: http://proceedings.asmedigitalcollection.asme.org/ on 06/19/2018 Terms of Use: http://www.asme.org/about-asme/terms-of-use

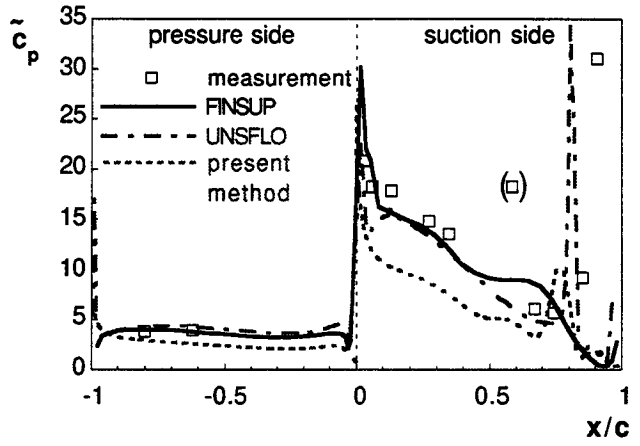

Fig. 3: Unsteady pressure coefficient on the blade "0" for measurement and all three flow solvers

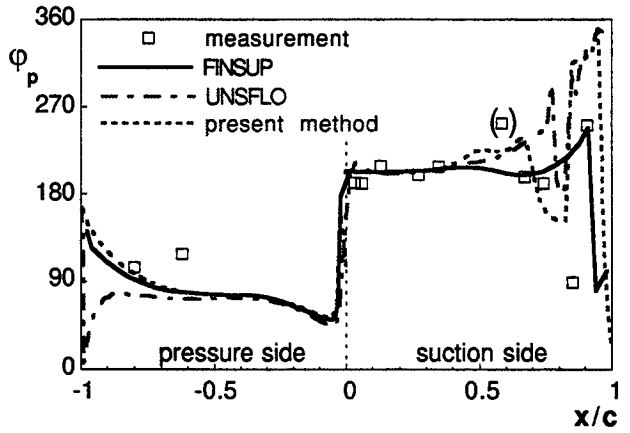

Fig. 4: Phase angle between unsteady pressure and blade movement of blade "0" for measurement and all three flow solvers

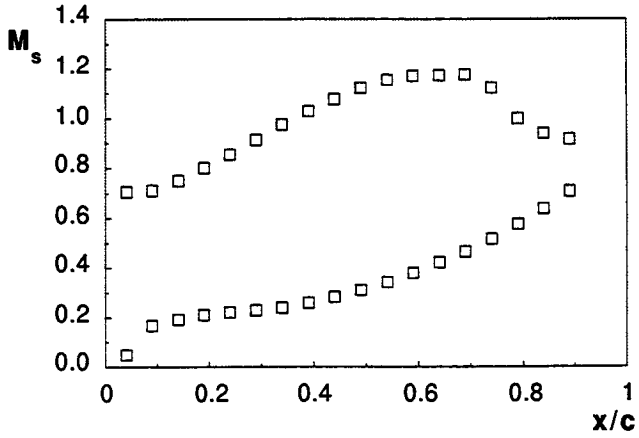

Fig. 5: Measured isentropic blade surface Mach number

Figure 6 presents a flow visualization during the test using the Schlieren technique. On the suction side of blade "+1" the normal shock is situated at 75 % of the chord length. Also it can be seen in this figure that the flow is not perfectly periodic, since periodicity is very difficult to achieve for transonic flows. The shock on the blade "0" is situated at about 90 % of the chord length.

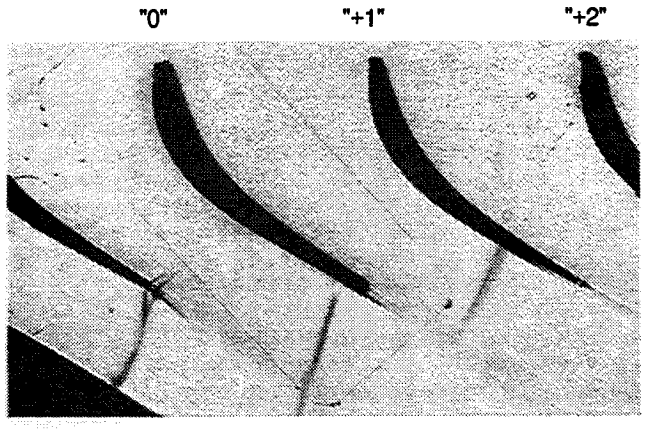

Fig. 6: Schlieren flow visualization

RESULTS AND DISCUSSION

Measurements

Steady-State Flow

Figure 5 shows the isentropic Mach number distribution measured on blade "1". On the suction side an acceleration up to about 60 % of the chord length can be observed up to a maximum speed of $M_s = 1.2$. Subsequently a zone with almost constant speed exists which is terminated by a normal shock situated at about 75 % of the chord length.

Unsteady Flow

Figs. 7 and 8 summarize the measured values for the unsteady pressure coefficient and the phase angle measured on blade "0". Two values on the suction side are remarkable:

At about 60 % of the chord length a high pressure value was found as is usually only measured close to a shock. During these measurements the shock was situated between 75 % (blade "+1") and 90 % (blade "0") of the chord length and cannot explain this value. Thus, this value might indicate a measurement error and should not be used for comparisons.

The second large value is situated at about 90 % and is supposed to be due to the normal shock. However, the value of the pressure amplitude measured is about three times higher than measurements in an annular cascade for the same profile geometry and flow conditions shown.

Downloaded From: http://proceedings.asmedigitalcollection.asme.org/ on 06/19/2018 Terms of Use: http://www.asme.org/about-asme/terms-of-use

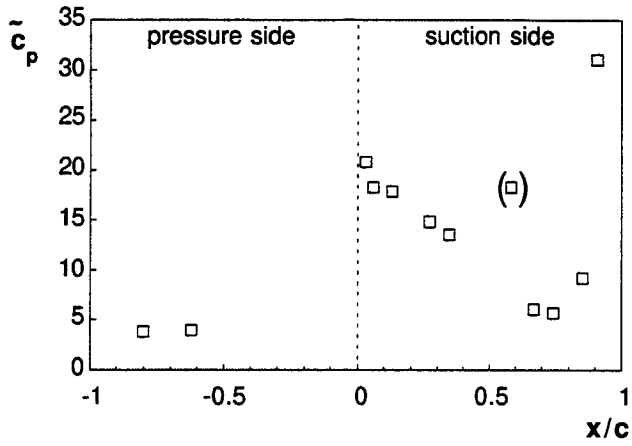

Fig. 7: Unsteady pressure coefficient on the blade surface of blade "0"

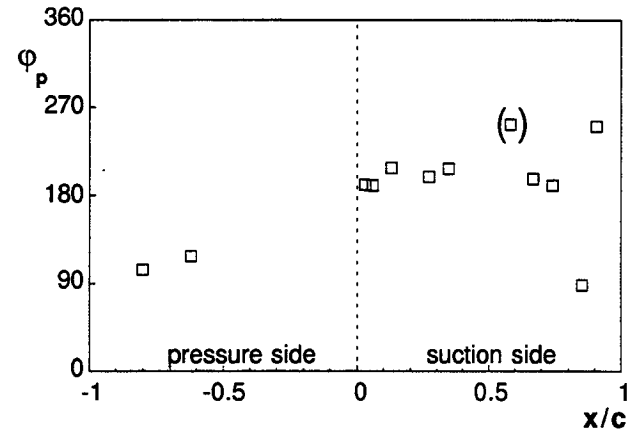

Fig. 8: Phase angle between unsteady pressure and blade movement of blade "0"

Computation

Steady-State Flow

For the steady-state computations, an iteration of the back pressure was undertaken with the objective of placing the shock at the same position that was found during the measurements.

The computational mesh for both calculations was identical with exception of the choice of the boundary condition in the outlet region: in the first computation the periodic boundary condition was used at the lateral up- and downstream boundaries, for the second computation the solid wall boundary condition was used at the downstream lateral boundaries to simulate the tailboards.

Table 1 gives an overview of the overall steady-state flow conditions during the measurements and for the computations.

		measurement	periodic boundary computation	tailboard computation
β_1	[°]	10.5	10.5	10.5
M_1	[-]	0.34	0.32	0.32
β_2	[°]		-58.7	-58.7
M_{2s}	[-]	0.94	0.93	0.92
p_2/p_{w1}	[-]	0.566	0.570	0.580

Table 1: *Overall steady-state flow conditions for measurements and computations*

Fig. 9 shows the comparison between the measured and computed blade surface Mach number distribution. As can be seen both computations give almost identical results and both compare very well with the measured values. The position and strength of the normal shock is identical for all cases.

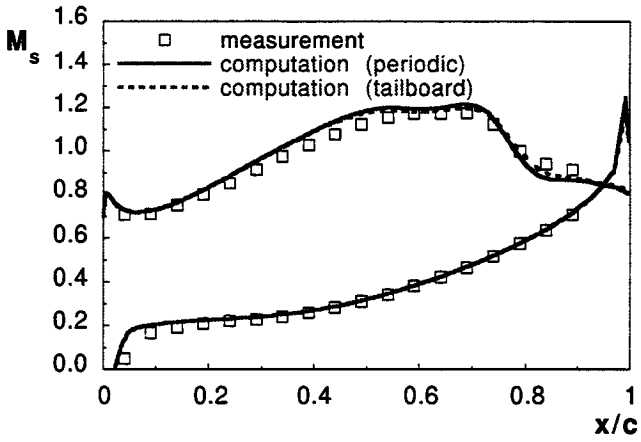

Fig. 9: Isentropic blade surface Mach number for measurement and both computations

Figs. 10 and 11 show the Mach numbers in the flow field for both computations. Fig. 10 which presents the case with periodic downstream lateral boundary conditions shows a perfectly periodic flow field. Fig. 11 shows the case with simulated tailboards and indicates that the flow field is aperiodic.

Figs. 12 and 13 present Schlieren pictures which were derived from the computational results. They show clearly that the shocks are not identical for the case with simulated tailboards and that the flow is aperiodic.

Downloaded From: http://proceedings.asmedigitalcollection.asme.org/ on 06/19/2018 Terms of Use: http://www.asme.org/about-asme/terms-of-use

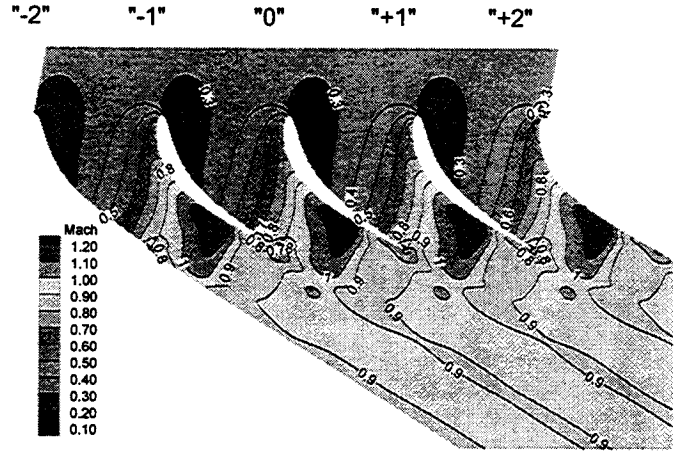

Fig. 10: Mach number distribution in the flow field for the computation with periodic downstream lateral boundaries

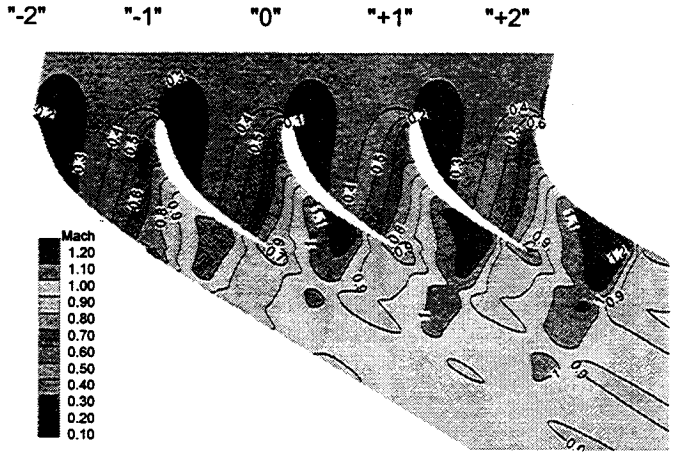

Fig. 11: Mach number distribution in the flow field for the computation with simulated tailboards

For this computation the shock on the suction side of blade "+2" is the strongest and the shock on the suction side of blade "-2" is the weakest shock. In Fig. 6, the Schlieren picture shows that the strongest shock is situated between the trailing edge of blade "-1" and the tailboard. This implies that the angle of the tailboards during the testing was set slightly differently than for the computation.

While looking for the outlet flow conditions which correspond to the correct blade Mach numbers, several computations for different outlet pressures and tailboard positions were carried out. The flow is very sensitive to the outlet flow angle and only a slight modification of the tailboard angle was necessary to obtain the same flow conditions. Therefore the abovementioned difference between the tailboard position during the measurement and during the computation was very small.

A comparison between Figures 6 and 13 shows that the periodicity, in terms of shock position, was better achieved during the computations than during the measurements.

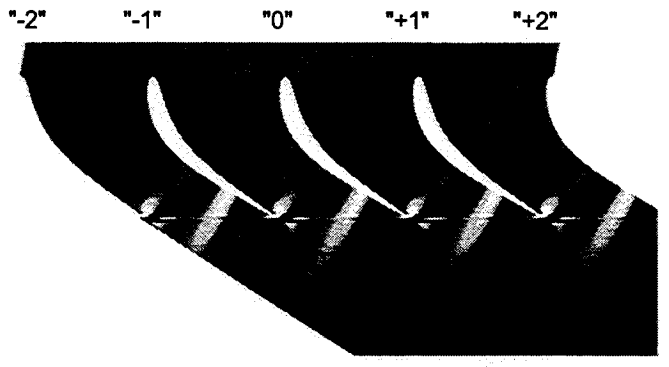

Fig. 12: "Schlieren picture" for the computation with periodic downstream lateral boundaries

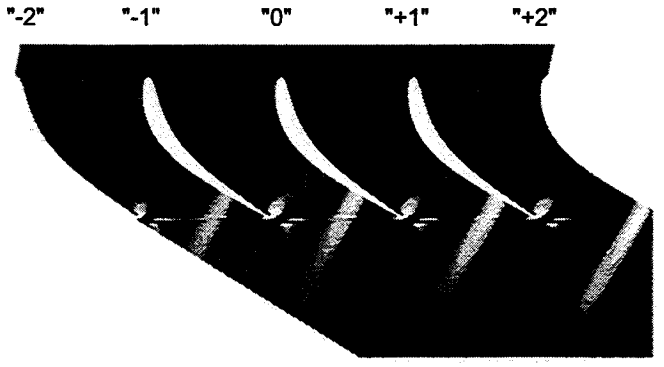

Fig. 13: "Schlieren picture" for the computation with simulated tailboards

Downloaded From: http://proceedings.asmedigitalcollection.asme.org/ on 06/19/2018 Terms of Use: http://www.asme.org/about-asme/terms-of-use

Unsteady Flow

The unsteady computations were conducted using the aforementioned steady-state solutions. The same vibration behavior (reduced frequency, dimensionless vibration amplitude, vibrating direction) as during the measurements was imposed. A number of vibration periods were computed until a periodic unsteady solution was achieved. Figures 14 and 15 show a comparison between the measured values and the computational results of both program versions.

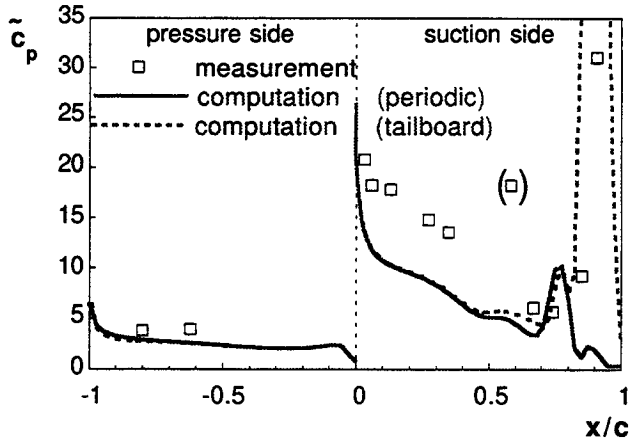

Fig. 14: Unsteady pressure coefficient on the blade surface of blade "0" for measurement and both computations

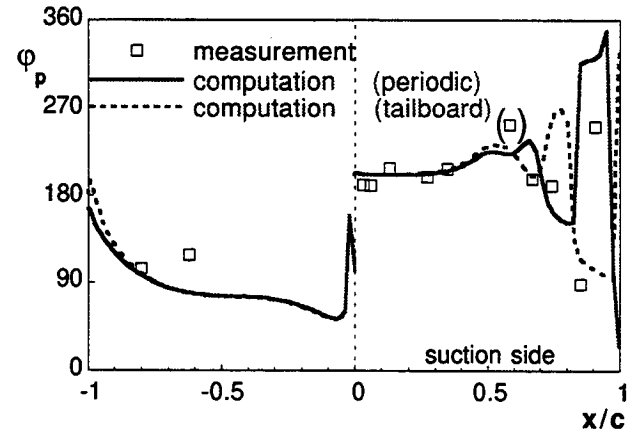

Fig. 15: Phase angle between unsteady pressure and blade movement of blade "0" for measurement and both computations

Both program versions generally underestimate the pressure amplitudes.

On the pressure side both versions of the program show an almost identical behavior for the pressure amplitude and the phase angle. There is a small difference as compared to the measured values especially with regards to the phase angle.

On the suction side both solvers show identical results up to about 50 % of the chord length for both pressure coefficient and phase angle. Both program versions predict similarly the increase of the unsteady pressure at the position of the shock at 75 % of the chord length. Behind this position the program version with simulated tailboards shows an extremely high pressure amplitude very close to the trailing edge which cannot be observed in the results with periodic downstream flow. The position of this very large amplitude coincides with the position on the blade where during the measurements the highest pressure amplitude was observed. This cannot be completely justified by the presence of the shock, since measurements on an annular cascade with an identical blade profile and the same flow conditions showed a considerably smaller unsteady pressure amplitude at that position. Thus, it is suspected that this large amplitude is due to the influence of the tailboards.

The two program versions produce significantly different results close to the trailing edge. The results of the version with the modeled tailboards are close to the measured values.

The presence of the tailboard seems to create some unsteady excitation which cannot be observed in the steady-state flow field. Since an inviscid computational method was capable of reproducing these effects, a possible conclusion is that the perturbations are most likely reflections of pressure waves.

CONCLUSIONS

Unsteady measurements in a linear test facility with one oscillating blade were realized for transonic outlet flow conditions. Comparisons with a computational program for unsteady flows through vibrating cascades showed discrepancies in the unsteady flow field even with almost identical blade surface Mach numbers.

The computational program was adapted for non-periodic flow by the introduction of solid guide walls (tailboards) in the downstream region. To match the experimental setup, four blade channels (five blades) were computed with only the middle blade vibrating.

Both computations give almost identical steady-state Mach number distributions on the blade surface of the center blade and compare very well with the measured distribution.

Nevertheless the computed flow fields show differences between both program versions and a non-periodicity in the case with simulated tailboards can be observed.

The difference between both computations is the presence of a tailboard. The result of the computation simulating tailboards is closer to the meaured values than the solution with periodic downstream lateral flow boundary condition. This leads to the conclusion that the observed unsteady excitations are created by the tailboards. Since the inviscid computational method was capable of reproducing these effects, the observed large pressure fluctuations are most likely due to pressure waves reflected on the tailboards.

Thus, computations for 'infinite cascades' cannot be applied to a linear cascade without concerns about reflections on the tailboards.

For steady-state measurements porous tailboards can eliminate or at least decrease the influence of the reflections, but for these unsteady measurements the slotted tailboards created additional harmonic perturbations and had to be replaced by solid tailboards.

For all measurements using a linear cascade, the existence of periodicity has to be examined extremely carefully, especially if unsteady measurements are to be performed.

Downloaded From: http://proceedings.asmedigitalcollection.asme.org/ on 06/19/2018 Terms of Use: http://www.asme.org/about-asme/terms-of-use

ACKNOWLEDGMENTS

The measurements were taken during a joint project with Rolls Royce plc, United Kingdom, ABB Power Generation Ltd., Switzerland, Volvo Flygmotor, Sweden and the Royal Institute of Technology in Stockholm, Sweden. The authors wish to thank all partners for their collaboration.

REFERENCES

Anderson, W.K.; Thomas, J.L.; van Leer, B.; 1987
"A Comparison of Finite Volume Flow with Shock Waves"
AIAA Paper 87-1152

Bölcs, A.; Fransson, T.H.; 1986
"Aeroelasticity in Turbomachines: Comparison of Theoretical and Experimental Cascade Results"
Communication du LTT N° 13, EPF-Lausanne, Switzerland

Bölcs, A.; Norryd, M.; 1994
"Development of a Sealing Construction to Prevent Leakage Flow During Flutter Tests in a Linear Cascade"
12th Symposium on Measuring Techniques for Transonic and Supersonic Flow in Cascades and Turbomachines, Prague, Czech Republic, 12-13 September 1994

Buffum, D.H.; Fleeter, S.; 1993
Effect Of Wind Tunnel Acoustic Modes On Linear Oscillating Cascade Aerodynamics
Proceedings of the 38th International Gas Turbine and Aeroengine Congress, Cincinnati, Ohio, May 24-27, 1993, Paper 93-GT-149

Fransson, T.H.; Verdon, J.M.; 1992
"Updated report on 'Standard Configurations for Unsteady Flow Through Vibrating Axial-Flow Turbomachine-Cascades', Status as of July 1991"
TRITA/KRV/92-009, KTH-Stockholm, Sweden

Fransson, T.H.; Jöcker, M.; Bölcs, A.; Ott, P.; 1998
"Viscous and Inviscid Linear/Nonlinear Calculations Versus Quasi 3D Experimental Data for a New Aeroelastic Turbine Standard Configuration"
Submitted to the ASME Gas Turbine and Aeroengine Congress - June 2-5, 1998 - Stockholm, Sweden

Girault, J.P. 1984
"Le flottement de flexion en régime supersonique amorcé"
La recherche aérospatiale, Année 1984, n° 1 (Janvier-Février), pp. 57-66

Loiseau, H.; Széchényi, E.; 1981
"Aéroélasticité des aubes de compreseurs - Étude du flottement de décrochage subsonique"
La recherche aérospatiale, Année 1981, n° 6 (Novembre-Décembre), p. 393-404

Norryd, M.; 1997
"Experimental Investigation of Unsteady Flow Effects including Tip Clearance in a Turbine Cascade"
Thèse N°1661, EPF-Lausanne, Switzerland

Ott, A.; Bölcs, A.; Fransson, T.H.; 1995
"Experimental and Numerical Study of the Time-Dependent Pressure Response of a Shock Wave Oscillating in a Nozzle"
Journal of Turbomachinery, January 1995, Vol. 117, p. 106 – 114

Schläfli, D.; 1989
"Experimentelle Untersuchung der instationären Strömung in oszillierenden Ringgittern"
Thèse N° 800, EPF-Lausanne, Switzerland

Rolls Royce plc; 1987
"FINSUP, User Guide and Reference Manual"
Rolls Royce commercial technology, Derby, England

Rolls Royce plc, M. Giles; 1991
"UNSFLO: A Numerical Method for the Calculation of Unsteady Flow in Turbomachinery"
Rolls Royce, GTL Report No 205, Derby, England

Széchényi, E.; Girault, J.P. 1981
"A study of compressor stall flutter in a straight wind tunnel"
Aeroelasticity in Turbomachines, Proceedings of the Second International Symposium held in Lausanne, September 8-12, 1980, Editor: P. Suter

Széchényi, E.; Cafarelli, I. 1989
"Le flottement des aubes de compresseur: Une certaine compréhension grâce à des essais en soufflérie"
Revue Française de Mécanique N° 1, 1989, pp. 73-87

Downloaded From: http://proceedings.asmedigitalcollection.asme.org/ on 06/19/2018 Terms of Use: http://www.asme.org/about-asme/terms-of-use